Geophysical Research Letters

RESEARCH LETTER
10.1002/2017GL076813

Solar Wind Deflection by Mass Loading in the Martian Magnetosheath Based on MAVEN Observations

E. Dubinin[1], M. Fraenz[1], M. Pätzold[2], J. S. Halekas[3], J. Mcfadden[4], J. E. P. Connerney[5], B. M. Jakosky[6], O. Vaisberg[7], and L. Zelenyi[7]

[1]Max-Planck-Institute for Solar System Research, Göttingen, Germany, [2]Rheinisches Institut fuer Umweltforschung, Abteilung Planetforschung, Cologne, Germany, [3]Department of Physics and Astronomy, University of Iowa, Iowa City, IA, USA, [4]Space Sciences Laboratory, University of California, Berkeley, CA, USA, [5]NASA Goddard Space Flight Center, Greenbelt, MD, USA, [6]Laboratory for Atmospheric and Space Physics, University of Colorado Boulder, Boulder, CO, USA, [7]Institute of Space Research, Moscow, Russia

Key Points:
- Due to interaction with the oxygen atmosphere the shocked solar wind is deflected
- The solar wind flow around Mars becomes asymmetrical
- The occurrence of deflection can be described by the multifluid MHD equation simplying mass-loading processes

Correspondence to:
E. Dubinin,
dubinin@mps.mpg.de

Citation:
Dubinin, E., Fraenz, M., Pätzold, M., Halekas, J. S., Mcfadden, J., Connerney, J. E. P., et al. (2018). Solar wind deflection by mass loading in the Martian magnetosheath based on MAVEN observations. *Geophysical Research Letters*, *45*. https://doi.org/10.1002/2017GL076813

Received 14 DEC 2017
Accepted 23 FEB 2018
Accepted article online 5 MAR 2018

Abstract Mars Atmosphere and Volatile EvolutioN observations at Mars show clear signatures of the shocked solar wind interaction with the extended oxygen atmosphere and hot corona displayed in a lateral deflection of the magnetosheath flow in the direction opposite to the direction of the solar wind motional electric field. The value of the velocity deflection reaches ~50 km/s. The occurrence of such deflection is caused by the "Lorentz-type" force due to a differential streaming of the solar wind protons and oxygen ions originating from the extended oxygen corona. The value of the total deceleration of the magnetosheath flow due to mass loading is estimated as ~40 km/s.

Plain Language Summary Mars Atmosphere and Volatile EvolutioN observations at Mars show that the solar wind interaction with Mars occurs already far from the planet. We observe clear signatures of the interaction with the extended oxygen atmosphere displayed in a lateral deflection of the magnetosheath flow in the direction opposite to the direction of the solar wind motional electric field. In a certain sense Mars resembles a small comet with the already formed magnetospheric cavity and a bow shock.

1. Introduction

The absence of the global magnetic field at Mars leads to the direct interaction of solar wind with its atmosphere and ionosphere. The interaction starts at large distances from the planet because of the hydrogen atmosphere and the hot oxygen corona which extends to many Martian radii (Chaffin et al., 2014, 2015; Chaufray et al., 2008; Clarke et al., 2017; Deighan et al., 2015; Feldman et al., 2011). Signatures of such distant interaction are picked-up protons and oxygen ions observed in the upstream solar wind (Barabash et al., 1991; Curry et al., 2015; Dubinin, Fraenz, Woch, Barabash, et al., 2006; Rahmati et al., 2015, 2017; Yamauchi et al., 2015). Charge exchange between incoming solar wind protons and planetary hydrogen also forms a beam of energetic neutral atoms (Futaana et al., 2006; Gunell et al., 2006) which penetrate deep into the Martian atmosphere where they are partly converted back to energetic positively and negatively charged hydrogen atoms (Halekas et al., 2015).

Ionized hydrogen atoms are picked up by solar wind (Barabash et al., 1991; Dubinin, Fraenz, Woch, Barabash, et al., 2006). Due to their low mass, the momentum lost by the incoming solar wind is small, although the exospheric protons reflected from the bow shock can contribute to the population of backstreaming ions and participate in the processes of the momentum exchange with solar wind protons via wave-particle interaction (Dubinin & Fraenz, 2016; Dubinin et al., 1994; Mazelle et al., 2004). Oxygen ions originating in the solar wind and the magnetosheath are also picked up and move on cycloidal trajectories. Because of the small size of Mars as compared to the amplitude of these cycloids, oxygen ions are deflected and accelerated toward the hemisphere in which the solar wind motional electric field is pointing away from the Mars-Sun line (E^+ hemisphere). This ion motion provides an excess of transverse momentum in the system which must be balanced by the motion of the solar wind protons in the opposite direction. Forces responsible for such an ion motion are Lorentz-type forces which appear in bi(or multi)-ion magnetohydrodynamic (MHD) equations

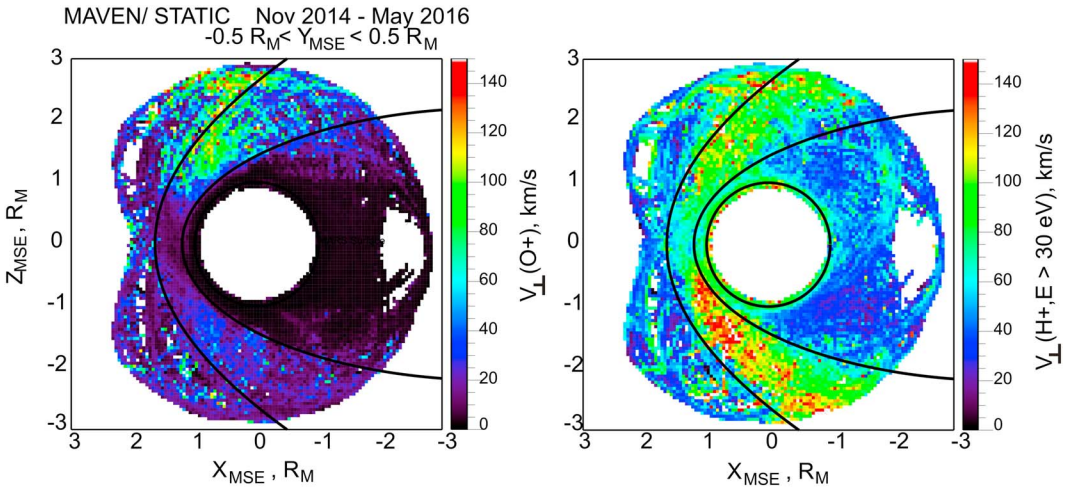

Figure 1. Maps of the cross-flow component of the ion velocities in the XZ_{MSE} cross section obtained from the Suprathermal and Thermal Ion Composition (STATIC) measurements at $-0.5\ R_M \le Y_{MSE} \le 0.5\ R_M$. The left (right) panel depicts the velocity of O^+ (H^+) ions, respectively. Solid curves correspond to the nominal position of the Martian bow shock and the magnetospheric boundary (Dubinin, Fraenz, Woch, Barabash, et al., 2006).

(Dubinin & Sauer, 1999, Dubinin et al., 2011; Harold & Hassam, 1994; Sauer et al., 1994). As compared to a single fluid MHD, in a bi-ion MHD approach, new Lorentz-type terms appear in the momentum equations:

$$m_p \frac{d\boldsymbol{u}_p}{dt} = \frac{\boldsymbol{j}\times\boldsymbol{B}}{n_e} + e\frac{n_{O^+}}{n_e}(\boldsymbol{V}_p - \boldsymbol{V}_{O^+})\times\boldsymbol{B} \quad (1)$$

$$m_{O^+} \frac{d\boldsymbol{u}_{O^+}}{dt} = \frac{\boldsymbol{j}\times\boldsymbol{B}}{n_e} + e\frac{n_p}{n_e}(\boldsymbol{V}_{O^+} - \boldsymbol{V}_p)\times\boldsymbol{B}, \quad (2)$$

where m_p, m_{O^+}, n_p, n_{O^+}, V_p, and V_{O^+} are masses, densities, and velocities of the protons and oxygen ions, respectively; n_e is the electron density; and $\boldsymbol{j}$ and $\boldsymbol{B}$ are the current density and the magnetic field, respectively. The Lorentz force caused by a differential streaming of ion fluids acts on the protons and oxygen ions in the opposite directions. This effect can be easily explained by noting that each ion fluid in their reference frame "sees" the motional electric field of the opposite sign. For example, when protons move faster than oxygen ions and consequently faster than the electrons which supply a quasineutrality, the motional electric field in the proton frame $\boldsymbol{E} = -(\boldsymbol{V}_e - \boldsymbol{V}_p)\times\boldsymbol{B}$ is opposite to the motional electric field in the frame related with the motion of O^+ ions, $\boldsymbol{E} = -(\boldsymbol{V}_e - \boldsymbol{V}_{O^+})\times\boldsymbol{B}$. Thus, neglecting the $\boldsymbol{j}\times\boldsymbol{B}$ term, which might be valid for a weak mass loading, causes the proton fluid to also move along a cycloid with a characteristic length $\sim V_p/(\frac{eB}{m_p}\frac{n_{O^+}}{n_e})$ which varies with the density of O^+ ions and might be very large for low densities of oxygen ions (Dubinin et al., 2011). As long as $(\boldsymbol{V}_p - \boldsymbol{V}_{O^+})\cdot\boldsymbol{V}_p \ge 0$, the work performed by the proton fluid is positive; that is, protons transfer the momentum to the ion oxygen fluid.

Halekas, Ruhunusiri, et al. (2017) have observed a small lateral deviation of the solar wind velocity (~5 km/s) in the direction opposite to the direction of the motional electric field indicating a weak mass-loading effect upstream of the bow shock. One may expect that closer to Mars mass-loading effects exposed in the solar wind deflection should be more pronounced. However, in contrast to weak comets where the solar wind is deflected up to 90° and then even turns to the sunward direction (Behar et al., 2017), the situation at Mars is very different since the bow shock causes a strong deflection of the plasma flow around the magnetospheric obstacle. The goal of this paper is to do a study on an asymmetry in the solar wind flow in the magnetosheath that appeared due to mass-loading effects.

2. Observations

The measurements made by the Mars Atmosphere and Volatile EvolutioN (MAVEN) spacecraft give us the opportunity to study these processes (Jakosky et al., 2015). In this paper we use the data from the Solar Wind

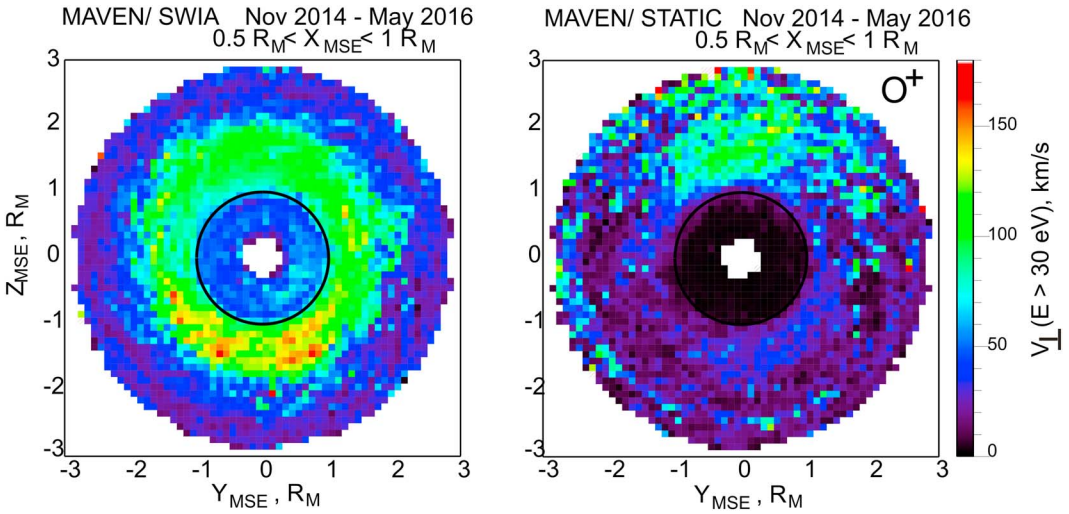

Figure 2. Maps of the mean cross-flow component of the proton velocity measured by Solar Wind Analyzer (SWIA) and oxygen ions measured by Suprathermal and Thermal Ion Composition (STATIC) in the YZ_{MSE} cross sections at the distance 0.5 $R_M \leq X \leq 1$ R_M.

Analyzer (SWIA), the Suprathermal and Thermal Ion Composition (STATIC) instrument, and the magnetometer MAG. The SWIA is a top-hat electrostatic analyzer measuring ions with energies 30 eV to 25 keV with 360° × 90° field of view and 4 s time resolution (Halekas et al., 2015). With its field of view toward the Sun the instrument is monitoring solar wind. We used here the onboard calculated moments of the ion distribution functions. Although in the magnetosheath more coarse distributions with incomplete coverage of the phase space are returned to the telemetry, the observations by SWIA provide an adequate solar wind flow behind the bow shock (see details in Halekas, Ruhunusiri, et al., 2017). The STATIC analyzer is able to measure different ion species (McFadden et al., 2015). It also consists of a toroidal top-hat electrostatic spectrometer with field of view of 360° × 90° combined with a time-of-flight unit able to resolve the major ion species (H^+, He^{++}, He^+, O^+, O_2^+, and CO_2^+). To decrease the contribution of protons scattered in the analyzer onto the oxygen mass channel, we subtracted 3% of counts measured in the proton channel at each energy step. The magnetic field is measured by two tri-axis fluxgate magnetometers (Connerney et al., 2015). We utilize the magnetic field data to determine the Mars Solar Electric (MSE) coordinate system in which the *X* axis is toward the Sun, the *Y* axis is along the cross-flow component of the magnetic field in the solar wind, and the *Z* axis points along the solar wind motional electric field. We utilize the MAVEN data from November 2014 to May 2016.

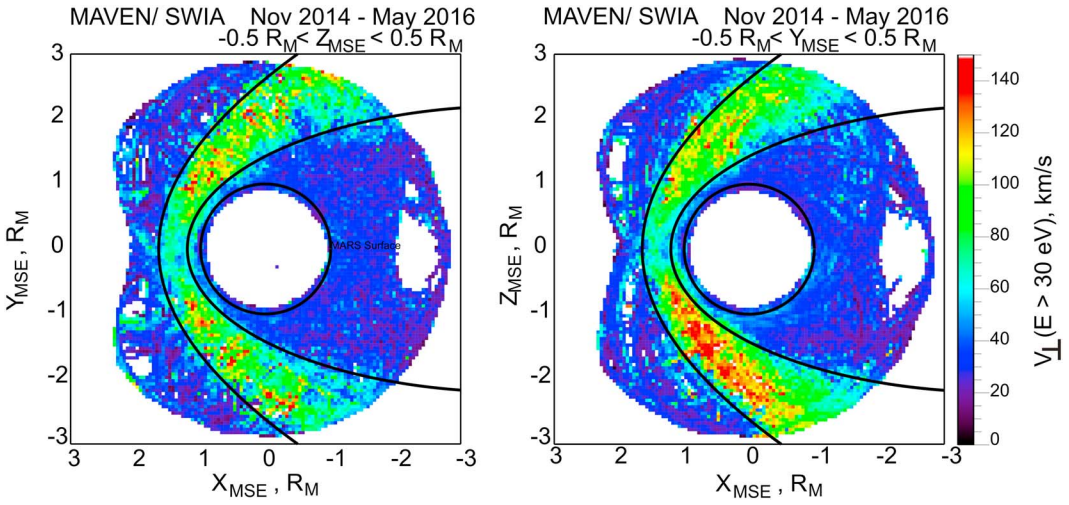

Figure 3. Maps of the mean transverse components of the proton velocity measured by Solar Wind Analyzer (SWIA) in the horizontal XY_{MSE} and vertical XZ_{MSE} cross sections.

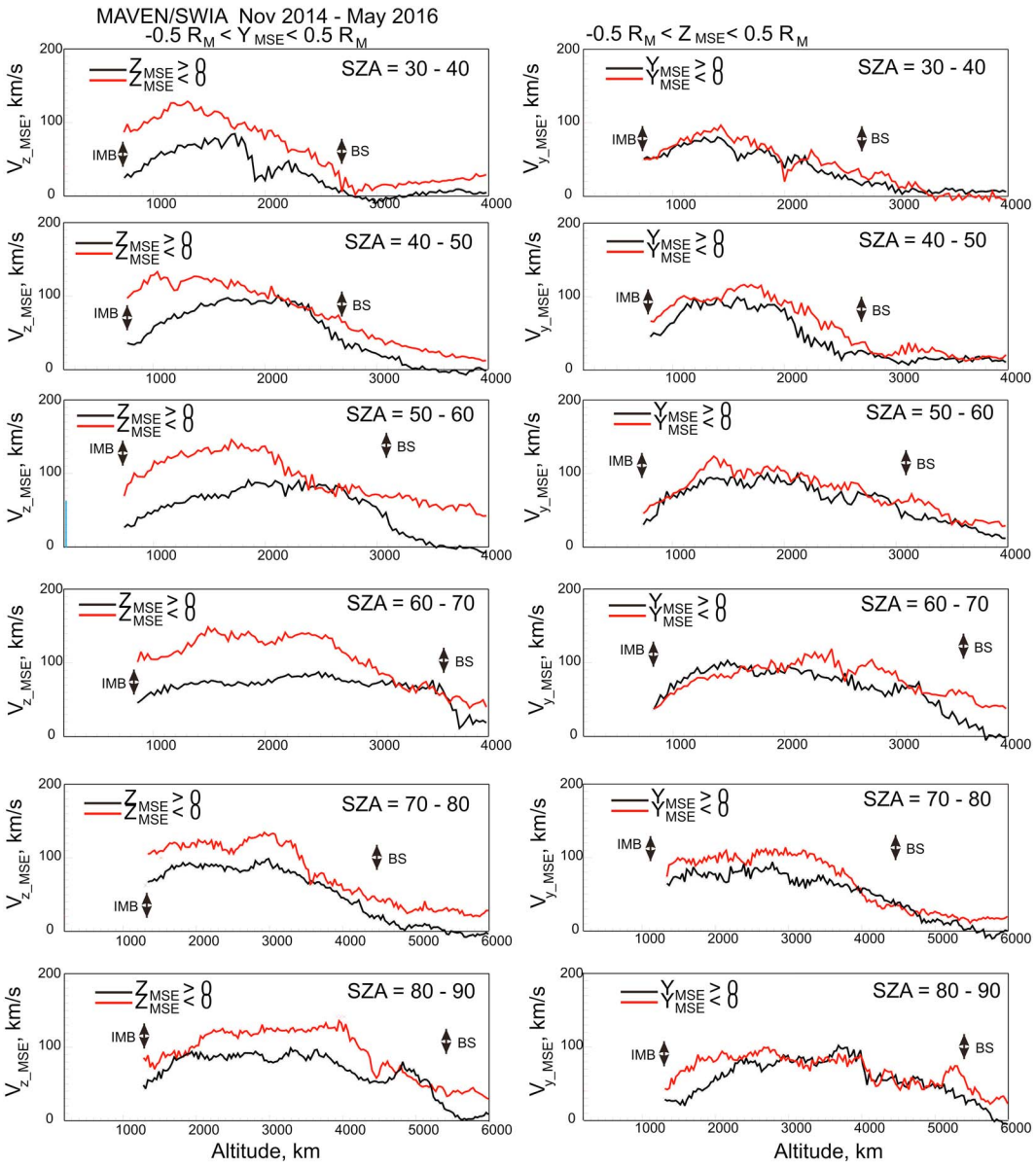

Figure 4. Altitude profiles of the absolute values of the components of the mean proton velocities V_Z and V_Y in the Mars Solar Electric (MSE) coordinate system measured by Solar Wind Analyzer (SWIA) at different solar zenith angles (SZA) in the XZ_{MSE} (left column) and XY_{MSE} (right column) planes, respectively. In the XZ_{MSE} plane black and red curves depict the absolute value of the mean V_Z component in the E^+ and E^- hemispheres, respectively. In the XY_{MSE} plane the black and red curves show the horizontal velocity in the +/− Y direction, respectively. Note the difference in values of the horizontal axis for two bottom rows. Nominal positions of the bow shock and the induced magnetospheric boundary are shown by arrows.

To observe a lateral deflection caused by the interaction of shocked solar wind with the population of oxygen ions, we have to compare deflections of the solar wind protons in the E^+ and the opposite E^- hemispheres. Figure 1 shows maps of the cross-flow component $(V^2_{Y_{MSE}} + V^2_{Z_{MSE}})^{1/2}$ of the ion velocities in the XZ_{MSE} cross section obtained from the STATIC measurements at $-0.5\,R_M \le Y_{MSE} \le 0.5\,R_M$. The left (right) panel depicts the velocity of O^+ (H^+) ions, respectively. For further comparison with the SWIA data, we calculated the moments by using the proton distributions with $E \ge 30$ eV. Solid curves correspond to the nominal position of the Martian bow shock and the magnetospheric boundary (Dubinin, Fraenz, Woch, Roussos, et al., 2006). A strong asymmetry of O^+ fluxes in the magnetosheath and in the adjacent upstream region appears due to large gyroradius of these ions as compared to the characteristic size of the system. Although the distribution of the cross-flow component of the proton velocity is more symmetrical due to a deflection of the solar wind

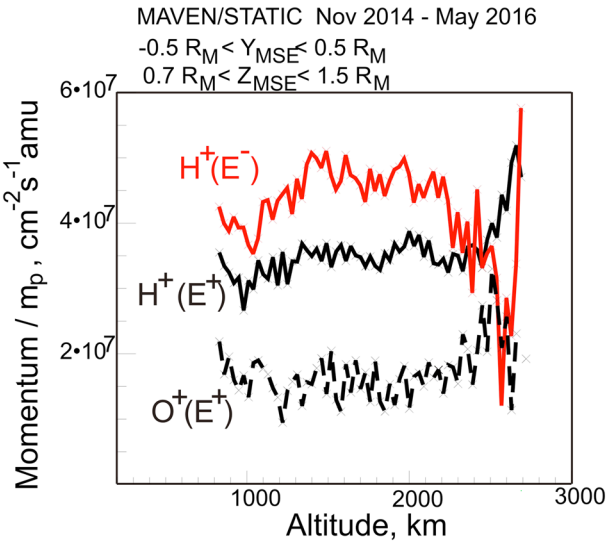

Figure 5. Z_{MSE} components of the momentum of the protons and O^+ ions in the E^+ and E^- sheath hemispheres.

at the bow shock, an asymmetry between E^+ and E^- hemispheres is observed. A stronger deflection occurs in the E^- hemisphere. A clear asymmetry between both magnetosheath hemispheres is also seen in Figure 2, which shows maps of the cross-flow component of the proton velocity measured by SWIA and oxygen ions measured by STATIC in YZ_{MSE} cross sections for the distance range $0.5\ R_M \le X \le 1\ R_M$. This range samples a significant fraction of the sheath.

Figure 3 compares the transverse components of the proton velocity measured by SWIA in the horizontal XY_{MSE} and vertical XZ_{MSE} cross sections. In the horizontal plane the plasma flow in the sheath is rather symmetrical, while in the vertical plane the proton flow deflects more strongly to the E^- hemisphere. These results are in agreement with the STATIC observations (see Figure 1).

Figure 4 shows the asymmetry between both hemispheres in more detail. It presents the altitude profiles of the absolute values of the components of the proton velocity $abs(V_{Z_{MSE}})$ and $abs(V_{Y_{MSE}})$ measured by SWIA at different solar zenith angles (SZA) in the XZ_{MSE} (left column) and XY_{MSE} (right column) planes, respectively. Nominal positions of the bow shock and the induced magnetospheric boundary are shown by arrows. In the XZ_{MSE} plane black and red curves depict the absolute values of the $V_{Z_{MSE}}$ component in the E^+ and E^- hemispheres, respectively. In the XY_{MSE} plane the black and red curves show the horizontal velocity $V_{Y_{MSE}}$ in +/− Y direction, respectively. A systematic shift of the proton flow in the direction opposite to the direction of the solar wind motional electric field is observed at all solar zenith angles indicating a mass loading of the solar wind by the oxygen corona. In the horizontal plane (XY_{MSE}) the proton flow is rather symmetrical. At certain SZA, we observe rather large values of the $abs(V_{Z_{MSE}})$ outside of the nominal position of the bow shock. It might be related to a rather high variability of the bow shock position (Halekas, Ruhunusiri, et al., 2017).

It is reasonable to assume that without a lateral shift of the proton flow due to the interaction with oxygen the deflection of solar wind at the bow shock would be axially symmetric. Then, with mass-loading effects, the value of the Z_{MSE} component of the velocity in the E^+ and E^- hemispheres are $V_Z^+ = V_{sym} - V_{ML_Z}$ and $V_Z^- = V_{sym} + V_{ML_Z}$, respectively. Here V_{sym} is the value of the velocity component due to symmetric deflection of the solar wind flow behind the bow shock, and V_{ML_Z} is the lateral velocity deflection (Z_{MSE} component) due to mass loading. Since the difference between V_Z^- and V_Z^+ reaches 60 km/s, the V_Z component of a lateral shift of the proton velocity in the magnetosheath is about 30 km/s. Correspondingly, the total component of a lateral velocity deflection in the sheath is $V_{def} \sim V_{ML_Z}/\cos\alpha$, where α is angle between the normal to the shocked solar wind trajectory in the magnetosheath and the vector $-Z_{MSE}$. Taking $\alpha \sim 45–60°$ yields $V_{def} \sim 43–60$ km/s. Then using equation (1) we can roughly estimate the deceleration of the protons by the "Lorentz" force:

$$\Delta u_p \sim \left(\frac{e}{m_p}\frac{n_{O^+}}{n_e}V_{def}BL\right)^{1/2}. \quad (3)$$

Taking $n_{O^+} \sim 0.1\ cm^{-3}$, $n_e \sim 10\ cm^{-3}$, $V_{def} \sim 50$ km/s, $B \sim 10$ nT, and $L \sim 1\ R_M$ (the characteristic length of the deceleration) yields $\Delta V_p \sim 40$ km/s. Here when utilizing equation (1) we considered the E^- hemisphere in which V_{def,O^+} is small and neglected the gradient of the thermal pressure and the $j \times B$ force, which is justified by Halekas, Brain, et al. (2017).

Conservation of the transverse momentum in the Z_{MSE} direction requires $m_p n_p V_{p_z}^+ + m_{O^+} n_{O^+} V_{O_z^+}^+ = m_p n_p V_{p_z}^-$. Figure 5 shows the values of these terms evaluated from the STATIC measurements in the E^+ sheath at $-0.5\ R_M \le Y_{MSE} \le 0.5\ R_M$ and $0.7\ R_M \le Z_{MSE} \le 1.5\ R_M$ and in the E^- sheath at $-0.5\ R_M \le Y_{MSE} \le 0.5\ R_M$ and $-1.5\ R_M \le Z_{MSE} \le -0.7\ R_M$. It is observed that the contribution of the term related to the oxygen motion approximately compensates for the deficit in the proton momentum in the E^+ hemisphere.

In conclusion, the MAVEN observations show that the solar wind interaction with Mars occurs already in the solar wind (Halekas, Ruhunusiri, et al., 2017) and in the magnetosheath. We observe clear signatures of the interaction with the extended oxygen atmosphere and hot corona displayed in a lateral deflection of the magnetosheath flow in the direction opposite to the direction of the solar wind motional electric field. The value

of the velocity deflection reaches ~50 km/s in the inner magnetosheath. The occurrence of such a deflection can be described by the multifluid MHD equations implying mass-loading processes in the system with large Larmour radius of the implanted planetary ions. In a certain sense Mars resembles a small comet with the already formed magnetospheric cavity and a bow shock.

Acknowledgments
The MAVEN project is supported by NASA through the Mars Exploration Program. MAVEN data are publicly available through the Planetary Data System. Authors E. D. and M. P. wish to acknowledge DFG for supporting this work by grant PA 525/14-1. Authors E. D. and M. F. wish to acknowledge support from DLR by grant 50QM1703. O. V. and L. Z. wish to acknowledge support from the Russian Science Foundation by grant 16-42-01 103.

References

Barabash, S., Dubinin, E., Pissarenko, N., Lundin, R., & Russell, C. T. (1991). Picked-up protons near Mars: Phobos observations. *Geophysical Research Letters*, *18*(10), 1805–1808. https://doi.org/10.1029/91GL02082

Behar, E., Nilsson, H., Alho, M., Goetz, C., & Tsurutani, B. (2017). The birth and growth of a solar wind cavity around a comet—Rosetta observations. *Monthly Notices of RAS*, *469*, S396–S403. https://doi.org/10.1093/mnras/stx1871

Chaffin, M., Chaufray, J. Y., Deighan, J., Schneider, N. M., McClintock, W. E., Stewart, A. I. F., et al. (2015). Three dimensional structure in the Martian H corona revealed by IUVS on MAVEN. *Geophysical Research Letters*, *42*, 9001–9008. https://doi.org/10.1002/2015/GL065287

Chaffin, M., Chaufray, J.-Y., Stewart, I., Montmessin, F., Schneider, N. M., & Bertaux, J.-L. (2014). Unexpected variability of Martian hydrogen escape. *Geophysical Research Letters*, *41*, 314–320. https://doi.org/10.1002/2013GL058578

Chaufray, J. Y., Bertaux, J. L., Leblanc, F., & Quémerai, E. (2008). Observation of the hydrogen corona with SPICAM on Mars Express. *Icarus*, *195*, 598–613. https://doi.org/10.1016/j.icarus.2008.01.009

Clarke, J. T., Mayyasi, M., Bhattacharyya, D., Schneider, N. M., McClintock, W. E., Deighan, J. I., et al. (2017). Variability of D and H in the Martian upper atmosphere observed with the MAVEN IUVS echelle channel. *Journal of Geophysical Research: Space Physics*, *122*, 2336–2344. https://doi.org/10.1002/2016JA023479

Connerney, J. E. P., Espley, J., Lawton, P., Murphy, S., Odom, J., Oliversen, R., & Sheppard, D. (2015). The MAVEN magnetic field investigation. *Space Science Reviews*, *195*(1–4), 257–291. https://doi.org/10.1007/s11214-015-0169-4

Curry, S. M., Luhmann, J. G., Ma, Y. J., Dong, C. F., Brain, D., Leblanc, F., et al. (2015). Response of Mars O^+ pickup ions to the 8 March 2015 ICME: Inferences from MAVEN data-based models. *Geophysical Research Letters*, *42*, 9095–9102. https://doi.org/10.1002/2015GL065304

Deighan, J., Chaffin, M. S., Chaufray, J.-Y., Stewart, A. I. F., Schneider, N. M., Jain, S. K., et al. (2015). MAVEN IUVS observation of the hot oxygen corona at Mars. *Geophysical Research Letters*, *42*, 9009–9014. https://doi.org/10.1002/2015GL065487

Dubinin, E., & Fraenz, M. (2016). Ultra-low-frequency waves at Venus and Mars. In A. Keiling, D.-H. Lee, & V. Nakariakov (Eds.), *Waves in space plasmas, Geophysical Monograph* (Vol. 216, pp. 343–364). Washington, DC: John Wiley. https://doi.org/10.1002/9781118842324.ch3

Dubinin, E., & Sauer, K. (1999). Martian magnetosphere—Laboratory for bi-ion plasma investigations. *Astrophysics and Space Science*, *264*, 273–288.

Dubinin, E., Fraenz, M., Fedorov, A., Lundin, R., Edberg, N., Duru, F., & Vaisberg, O. (2011). Ion energization and escape on Mars and Venus. *Space Science Reviews*, *162*, 173–211. https://doi.org/10.1007/s11214-011-9831-7

Dubinin, E., Fraenz, M., Woch, J., Barabash, S., Lundin, R., & Yamauchi, M. (2006). Hydrogen exosphere at Mars: Pickup protons and their acceleration at the bow shock. *Geophysical Research Letters*, *33*, L22103. https://doi.org/10.1029/2006GL027799

Dubinin, E., Fraenz, M., Woch, J., Roussos, E., Barabash, S., Lundin, R., et al. (2006). Plasma morphology at Mars: ASPERA-3 observations. *Space Science Reviews*, *126*, 209–238. https://doi.org/10.1007/s11214-006-9039-4

Dubinin, E., Obod, D, Pedersen, A., & Grard, R. (1994). Mass-loading asymmetry in upstream region near Mars. *Geophysical Research Letters*, *21*, 2769–2772.

Feldman, P. D., Steffl, A. J., Parker, J. W., A'Hearn, M. F., Bertaux, J.-L., Stern, S. A., et al. (2011). Rosetta-Alice observations of exospheric hydrogen and oxygen on Mars. *Icarus*, *214*, 394–399. https://doi.org/10.1016/j.icarus.2011.06.013

Futaana, Y., Barabash, S., Grigoriev, A., Holmström, M., Kallio, E., Brandt, P. C., et al. (2006). First ENA observations at Mars: ENA emissions from the Martian upper atmosphere. *Icarus*, *182*, 424–430.

Gunell, H., Brinkfeldt, K., Holmström, M., Brandt, P. C., Barabash, S., Kalliod, E., et al. (2006). First ENA observations at Mars: Charge exchange ENAs produced in the magnetosheath. *Icarus*, *182*(2), 431–438. https://doi.org/10.1016/j.icarus.2005.10.027

Halekas, J., Taylor, E., Dalton, G., Johnson, G., Curtis, D., McFadden, J., et al. (2015). The solar wind ion analyzer for MAVEN. *Space Science Reviews*, *195*, 125–151. https://doi.org/10.1007/s11214-013-0029-z

Halekas, J. S., Brain, D. A., Luhmann, J. G., DiBraccio, G. A., Ruhunusiri, S., Harada, Y., et al. (2017). Flows, fields, and forces in the Mars-solar wind interaction. *Journal of Geophysical Research: Space Physics*, *122*, 11,320–11,341. https://doi.org/10.1002/2017JA024772

Halekas, J. S., Ruhunusiri, S., Harada, Y., Collinson, G., Mitchell, D. L., Mazelle, C., et al. (2017). Structure, dynamics, and seasonal variability of the Mars-solar wind interaction: MAVEN solar wind ion analyzer inflight performance and science results. *Journal of Geophysical Research: Space Physics*, *121*, 547–578. https://doi.org/10.1002/2016JA023167

Harold, J. B., & Hassam, A. B. (1994). Two ion fluid numerical investigations of solar wind gas releases. *Journal of Geophysical Research*, *99*(A10), 19,325–19,340.

Jakosky, B. M., Lin, R. P., Grebowsky, J. M., Luhmann, J. G., Mitchell, D. F., Beutelschies, G., et al. (2015). The Mars Atmosphere and Volatile Evolution (MAVEN) mission. *Space Science Reviews*, *195*(1–4), 3–48. https://doi.org/10.1007/s11214-015-0139-x

Mazelle, C., Winterhalter, D., Sauer, K., Trotignon, J. G., Acuña, M. H., Baumgärtel, K., et al. (2004). Bow shock and upstream phenomena at Mars. *Space Science Reviews*, *11*, 115–181.

McFadden, J. P., Kortmann, O., Curtis, D., Dalton, G., Johnson, G., Abiad, R., et al. (2015). MAVEN Suprathermal and Thermal Ion Compostion (STATIC) instrument. *Space Science Reviews*, *195*, 199–256. https://doi.org/10.1007/s11214-015-0175-6

Rahmati, A., Larson, D. E., Cravens, T. E., Lillis, R. J., Dunn, P. A., Halekas, J. S., et al. (2015). MAVEN insights into oxygen pickup ions at Mars. *Geophysical Research Letters*, *42*, 8870–8876. https://doi.org/10.1002/2015GL065262

Rahmati, A., Larson, D. E., Cravens, T. E., Lillis, R. J., Halekas, J. S., McFadden, J. P., et al. (2017). MAVEN measured oxygen and hydrogen pickup ions: Probing the Martian exosphere and neutral escape. *Journal of Geophysical Research: Space Physics*, *122*, 3689–3706. https://doi.org/10.1002/2016JA023371

Sauer, K., Bogdanov, A., & Baumgaertel, K. (1994). Evidence of an ion composition boundary (protonopause) in bi-ion fluid simulations of solar wind mass loading. *Geophysical Research Letters*, *21*, 2255–2258. https://doi.org/10.1029/94GL01691

Yamauchi, M., Hara, T., Lundin, R., Dubinin, E., Fedorov, A., Sauvaud, J.-A., et al. (2015). Seasonal variation of Martian pick-up ions: Evidence of breathing exosphere. *Planetary and Space Science*, *119*, 54–61. https://doi.org/10.1016/j.pss.2015.09.013